Evolution of a band insulating phase from a correlated metallic phase

Kalobaran Maiti,* Ravi Shankar Singh, and V. R. R. Medicherla
Department of Condensed Matter Physics and Materials' Science, Tata Institute of Fundamental Research, Homi Bhabha Road, Colaba, Mumbai 400 005, India

(Received 24 September 2007; published 26 October 2007)

We investigate the evolution of the electronic structure in $SrRu_{1-x}Ti_xO_3$ as a function of x using high resolution photoemission spectroscopy, where $SrRuO_3$ is a weakly correlated metal and $SrTiO_3$ is a band insulator. Increase in x leads to an introduction of a local potential different from Ru-O sublattice. The features in the bulk spectra could be captured remarkably well using first principles approaches, and the electron correlation strengths are found to be similar in all the compositions. The surface spectra exhibit a metal-insulator transition at $x=0.5$ by opening up a soft gap at the Fermi level ϵ_F and a hard gap appears at higher x values. These results presumably provide an experimental demonstration of the predictions of metal-insulator transition due to local potential and electron correlation in a two-dimensional bipartite lattice using the ionic Hubbard model.

DOI: 10.1103/PhysRevB.76.165128 PACS number(s): 71.10.Hf, 71.20.−b, 71.30.+h

I. INTRODUCTION

The investigation of the role of electron correlation in various electronic properties is a paradigmatic problem in solid state physics. Electron correlation localizes the valence electrons leading the system toward insulating phase. Such correlation induced insulators, known as *Mott insulators*, are characterized by gapped electronic excitations in a system where effective single-particle approaches provide a metallic ground state. The *band insulators* represent insulating phase described within the effective single-particle approaches. Strikingly, some recent theoretical studies reveal a correlation induced metallic ground state in a band insulator using the ionic Hubbard model.[1–4] Such unusual transition has been observed in two dimensions by tuning U/W (U=electron-electron Coulomb repulsion strength, W=bandwidth) and the local potential Δ.

Here, we investigate the evolution of the electronic structure of $SrRu_{1-x}Ti_xO_3$ as a function of x. $SrRuO_3$ is a correlated ferromagnetic metal (T_C=165 K). Ti substitution introduces local potential different from Ru sites in the Ru-O sublattice (Ru-O sublattice determines the material properties in these systems). In $SrRu_{0.5}Ti_{0.5}O_3$, every alternative Ru site is replaced by a Ti site (unit cell is doubled) similar to a bipartite lattice considered in the ionic Hubbard model. Transport measurements[5] in this system in the form of thin films reveal a plethora of novel phases such as correlated metal ($x\sim0.0$), disordered metal ($x\sim0.3$), Anderson insulator ($x\sim0.5$), soft Coulomb gap insulator ($x\sim0.6$), disordered correlated insulator ($x\sim0.8$), and band insulator ($x=1.0$). Thus, this system is a good candidate to study the role of electron correlation and different local potential in exhibiting varieties of electronic properties.

We have used high resolution photoemission spectroscopy to probe the density function in the vicinity of the Fermi level ϵ_F and at higher energy scale as well. Since the escape depth of the photoelectrons is small, we have extracted the surface and bulk spectra in every case by varying the surface sensitivity of the technique. The bulk spectra exhibit an unusual spectral weight transfer and signature of a pseudogap at ϵ_F at higher x. Interestingly, the surface spectra of $SrRu_{1-x}Ti_xO_3$ exhibit a metal-insulator transition revealing a soft gap at ϵ_F for $x=0.5$ and a hard gap for higher x.

II. EXPERIMENT

Photoemission measurements were performed at 300 K using Gammadata Scienta analyzer SES2002 and monochromatized photon sources. The energy resolutions for x-ray photoemission (XP) and He II photoemission measurements were set at 300 and 4 meV, respectively. Sample surface was cleaned by scraping at 3×10^{-11} torr using diamond files. High quality samples of $SrRu_{1-x}Ti_xO_3$ with large grain size were prepared following solid state reaction route using high purity ingredients[6] followed by a long sintering (for about 72 h) in the highly pressed pellet form at the final preparation temperature. Sharp x-ray diffraction patterns reveal single phase in each composition with no signature of impurity feature. Magnetic measurements using a high sensitivity vibrating sample magnetometer exhibit distinct ferromagnetic transition at each x up to $x=0.6$ studied, as also evidenced by the Curie-Weiss fits in the paramagnetic region. The fits provide an estimation of the effective magnetic moment (μ=2.8, 2.54, 2.45, 2.18, 2.19, 1.95, and 1.93 μ_B) and Curie temperature (θ_P=164, 156.6, 150.6, 145.3, 139, 138.6, and 100 K) for x=0.0, 0.15, 0.2, 0.3, 0.4, 0.5, and 0.6, respectively. The values of μ and θ_P for $SrRuO_3$ are observed to be the largest among those available in the literature and correspond to well characterized single crystalline materials.[7]

III. RESULTS AND DISCUSSIONS

In Fig. 1(a), we show the integral background subtracted XP valence band spectra exhibiting four distinct features marked by A, B, C, and D. Features C and D represent density of states (DOS) having large O $2p$ character[8,9] and remain almost the same in the whole composition range as expected. Peaks A and B appear due to the electronic states having primarily Ru $4d$ character. While Ru $4d$ intensity gradually decreases with the decrease in Ru concentrations,

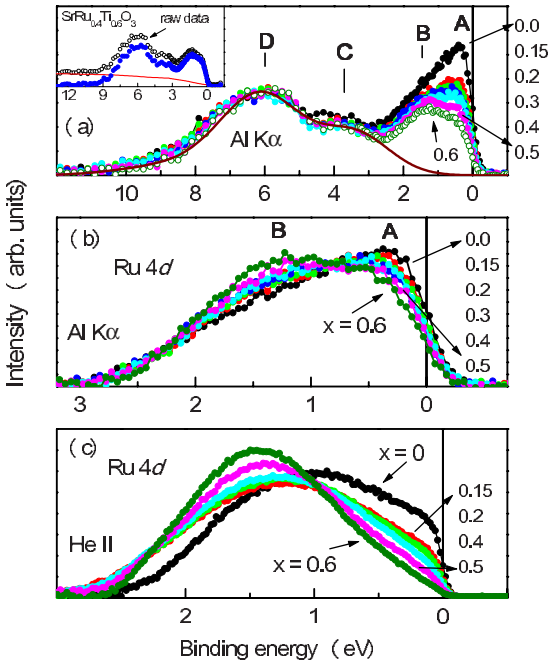

FIG. 1. (Color online) (a) Integral background subtracted XP valence band spectra of $SrRu_{1-x}Ti_xO_3$ for various values of x. Solid line represents the O $2p$ part for $x=0.6$. The inset demonstrates the background subtraction procedure. Open circles, solid line, and closed circles represent raw data and background and subtracted spectra of $SrRu_{0.4}Ti_{0.6}O_3$. (b) Ru $4d$ spectra after the subtraction of the O $2p$ contributions as shown in (a). (c) Ru $4d$ band obtained from He II spectra.

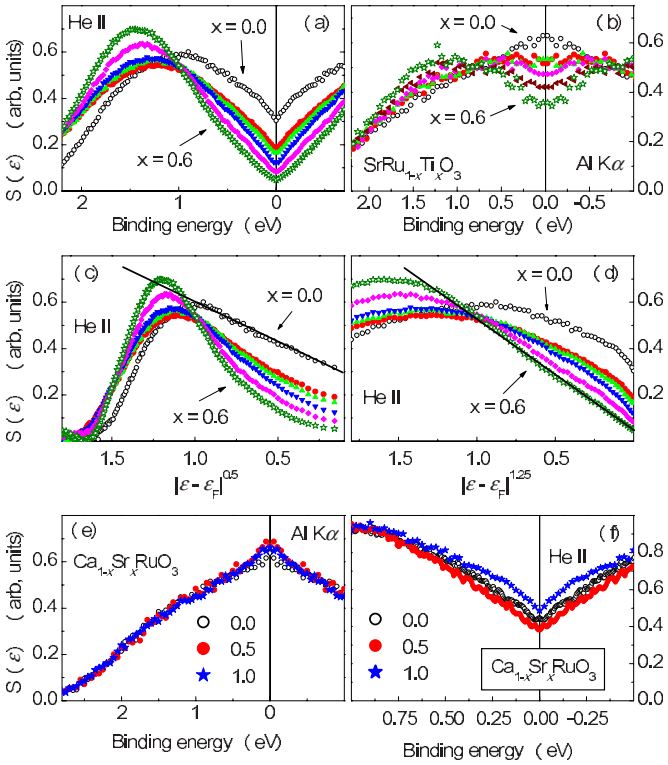

FIG. 2. (Color online) $S(\epsilon)$ obtained from (a) He II and (b) XP spectra of $SrRu_{1-x}Ti_xO_3$. (b) $S(\epsilon)$ in (a) are plotted as a function of (c) $|\epsilon-\epsilon_F|^{0.5}$ and (d) $|\epsilon-\epsilon_F|^{1.25}$. $S(\epsilon)$ obtained from (e) XP and (f) He II spectra of $Ca_{1-x}Sr_xRuO_3$.

the line shape of Ru $4d$ band exhibits significant redistribution in intensity. In order to bring out the clarity, we delineate the Ru $4d$ band by subtracting O $2p$ contributions at higher energies. The subtracted spectra are normalized by integrated intensity and shown in Fig. 1(b). Two features A and B are distinctly visible in the figure. Feature A corresponds to the delocalized DOS observed in *ab initio* results and is termed as *coherent feature*. Feature B, absent in the *ab initio* results,[9] is often attributed to the signature of correlation induced localized electronic states forming the lower Hubbard band and is known as *incoherent feature*. The increase in x leads to a significant change in line shape; relative intensity of A decreases and subsequently, the intensity of B grows gradually. Since the bulk sensitivity of valence electrons at 1486.6 eV photon energy is high ($\sim$60%), the spectral evolution in Fig. 1(b) manifests primarily in the changes in the bulk electronic structure.

In order to discuss the effect due to the surface electronic structure, we show the Ru $4d$ contributions extracted from the He II spectra in Fig. 1(c), where the surface sensitivity is about 80%. All the spectra are dominated by the peak at higher binding energies (>1 eV) corresponding to the surface electronic structure as also observed on thin film samples[10] and demonstrated in the case of $SrRuO_3$.[8,11] The coherent feature intensity reduces drastically with the increase in x and becomes almost negligible at $x=0.6$. This can be visualized clearly in the spectral density of states (SDOS) obtained by symmetrizing $[S(\epsilon)=I(\epsilon)+I(-\epsilon)$; $I(\epsilon)=$photoemission spectra, $\epsilon=$binding energy] the He II and XP spectra. The SDOS corresponding to He II spectrum of $SrRuO_3$ shown in Fig. 2(a) exhibits a sharp dip at ϵ_F, which increases gradually with the increase in x. The SDOS corresponding to XP spectra in Fig. 2(b), however, exhibits a peak in $SrRuO_3$ presumably due to large resolution broadening and intense coherent feature. This peak loses its intensity and becomes almost flat for $x=0.15$ and 0.2. Further increase in x leads to a pseudogap at ϵ_F, which gradually increases with the increase in x. Both these results clearly indicate gradual depletion of SDOS at ϵ_F with the increase in Ti substitution.

The effect of resolution broadening of 4 meV in the He II spectra is not significant in the energy scale shown in the figure. The electron and hole lifetime broadening is also negligible in the vicinity of ϵ_F. Thus, $S(\epsilon)$ in Fig. 2(a) provide a good testing ground to investigate evolution of the spectral line shape at ϵ_F. The line shape of $S(\epsilon)$ in Fig. 2(a) exhibits significant modification with the increase in x. We, thus, replot $S(\epsilon)$ as a function of $|\epsilon-\epsilon_F|^\alpha$ for various values of α. Two extremal cases representing $\alpha=0.5$ and 1.25 are shown in Figs. 2(c) and 2(d), respectively. It is evident that $S(\epsilon)$ of $SrRuO_3$ exhibit a straight line behavior in Fig. 2(c), suggesting significant role of disorder in the electronic structure. The influence of disorder can also be verified by substitutions at the A sites in the ABO_3 structure. This has been verified by plotting SDOS obtained from the XP and He II spectra of $Ca_{1-x}Sr_xRuO_3$ in Figs. 2(e) and 2(f), respectively. Here, the electronic properties of the end members, $SrRuO_3$ and

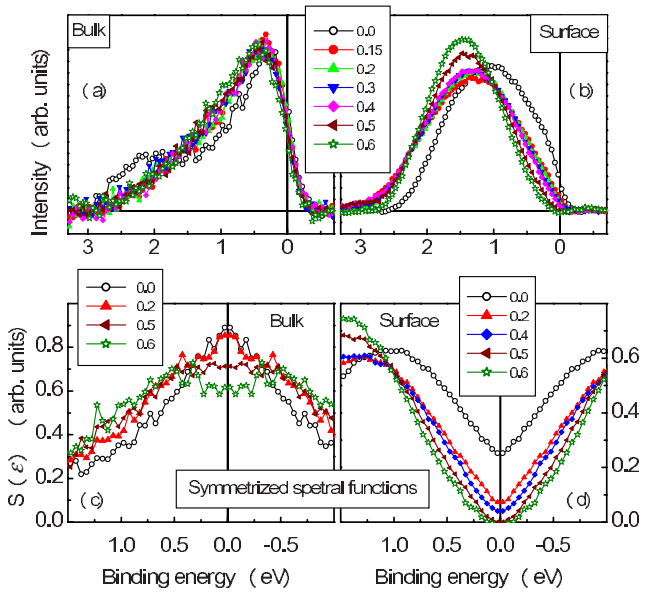

FIG. 3. (Color online) Extracted (a) bulk and (b) surface spectra of $SrRu_{1-x}Ti_xO_3$ for various values of x. The SDOs obtained from bulk and surface spectra are shown in (c) and (d), respectively.

$CaRuO_3$, are known to be strongly influenced by the disorder[12] presumably due to the defects and/or vacancies in the crystal lattice. Substitution of Sr at the Ca sites is expected to enhance the disorder effect. The line shape of $S(\epsilon)$ in both Figs. 2(e) and 2(f) remains almost the same across the whole composition range. Such disorder induced spectral dependence is consistent with the observations in other systems[13,14] as well.

The line shape modifies significantly with the increase in x and α becomes 1.25 in the 60% Ti substituted sample. In systems consisting of localized electronic states in the vicinity of ϵ_F, a soft Coulomb gap opens up due to electron-electron Coulomb repulsion; in such a situation, the ground state is stable with respect to single-particle excitations when SDOS is characterized by $(\epsilon-\epsilon_F)^2$ dependence.[15,16] Here, Ti substitution introduces defects in the Ru-O network, where Ti^{4+} having no d electron does not contribute in the valence band. In addition, the reduced degree of Ru-O-Ru connectivity leads to a decrease in bandwidth W and hence U/W enhances. Thus, gradual increase in α with the increase in x in the intermediate compositions is intriguing and indicates strong interplay between correlation effect and disorder in this system.

The extraction of surface and bulk spectra requires both the XP and He II spectra collected at significantly different surface sensitivities. Thus, we broaden the He II spectra up to 300 meV and extract the surface and bulk spectra analytically using the same parameters as used before for $CaSrRuO_3$ system.[8] The surface spectra shown in Fig. 3(b) exhibit a gradual decrease in coherent feature intensity with the increase in x, and subsequently, the feature around 1.5 eV becomes intense, narrower, and slightly shifted toward higher binding energies. The decrease in intensity at ϵ_F is clearly visible in the symmetrized spectra $S(\epsilon)$ shown in Fig. 3(d). Intensity at ϵ_F in $S(\epsilon)$ of $x=0.5$ sample becomes zero exhibiting a soft gap. A hard gap appears in $S(\epsilon)$ corresponding to higher x.

The spectral evolution in the surface spectra is remarkably consistent with the transport properties[5] measured on thin film materials, which has essentially two-dimensional symmetry. Although it is assumed that sufficiently thick films may correspond to the bulk of the material, it is often observed that substrate induced strain remains in the films even for large number of layers. This is presumably the reason why the magnetic ordering temperature observed for $SrRuO_3$ films is lower than that observed for bulk materials.[7]

Significantly different surface and bulk electronic structures have been observed in various $3d$ and $4d$ transition metal oxides.[8,17–20] This can be attributed primarily to three effects. (i) The crystal symmetry at the surface will be close to D_{4h} symmetry compared to the close to O_h symmetry observed in the bulk. Thus, the splitting of the Ru $4d$ bands will be stronger in the surface spectra. (ii) The absence of periodicity along the surface normal leads to significant narrowing of the valence band and, hence, the effective electron correlation strength will be enhanced at the surface. (iii) Surface reconstruction, defects, etc., also play significant role in determining the surface electronic structure.

While all the above factors are expected to be important, the evolution of the electronic structure in $SrRu_{1-x}Ti_xO_3$ will also be influenced by the introduction of difference in the local potential Δ between Ti and Ru sites due to Ti substitution in the Ru-O sublattice. Interestingly, the soft gap appears at $x=0.5$, where the system becomes similar to a bipartite lattice considered in the theoretical calculations.[1–4] Thus, these results corresponding to two-dimensional surface states presumably have strong implication in realizing recent theoretical predictions.

The picture is strikingly different in the bulk spectra where the electronic structure is three dimensional. The bulk spectrum of $SrRuO_3$ exhibits an intense and sharp coherent feature and the incoherent feature appears around 2 eV. The enhancement of U/W due to Ti substitution is expected to reduce the width of the coherent features along with an increase in the incoherent feature intensity. In sharp contrast, the coherent feature becomes significantly broad and appears very similar in the bulk spectra of all the intermediate compositions. The symmetrized bulk spectra shown in Fig. 3(c) exhibit a small lowering of intensity at ϵ_F with the increase in x.

Since U is weak in these highly extended $4d$ systems,[8,11] a perturbative approach may be useful to understand the role of electron correlation in the spectral line shape. We have calculated the bare density of states (DOS) for $SrRuO_3$ and $SrRu_{0.5}Ti_{0.5}O_3$ using state-of-the-art full potential linearized augmented plane wave method.[9,21] The self-energy and spectral functions were calculated using this t_{2g} partial DOS as done before.[22] The real and imaginary parts of the self-energy are shown in Figs. 4(a) and 4(b), and the spectral functions for different U values are shown in Figs. 4(c) and 4(d) for $SrRuO_3$ and $SrRu_{0.5}Ti_{0.5}O_3$, respectively. The increase in U leads to a spectral weight transfer outside the local-density approximation (LDA) DOS width, creating the lower and upper Hubbard bands. Subsequently, the total width of the LDA DOS diminishes gradually. While these

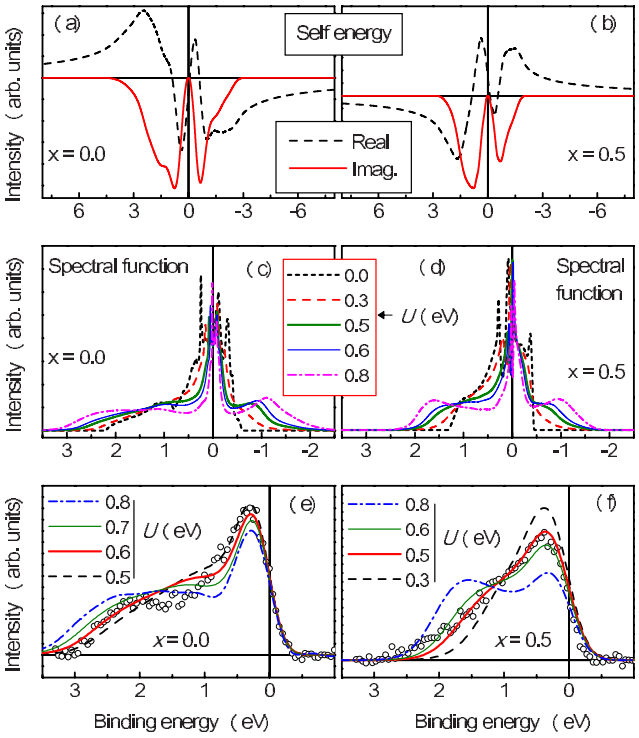

FIG. 4. (Color online) Real and imaginary parts of the self-energy of (a) $SrRuO_3$ and (b) $SrRu_{0.5}Ti_{0.5}O_3$ obtained by second order perturbation method following the method of Treglia *et al.* (Ref. 22). Spectral functions for various values of U of (c) $SrRuO_3$ and (d) $SrRu_{0.5}Ti_{0.5}O_3$. Calculated experimental spectra for different values of U of (e) $SrRuO_3$ and (f) $SrRu_{0.5}Ti_{0.5}O_3$.

results exhibit similar scenario as that observed in the most sophisticated calculations using dynamical mean field theory, the separation between the lower and upper Hubbard bands is significantly larger than the corresponding values of U. It is important to note here that the band structure calculations include the electron-electron interaction term within the local-density approximations. The perturbation calculations in the present case essentially provide an estimation of the correction in U already included in the effective single-particle Hamiltonian.

In order to compare with the experimental spectra, the calculated spectral functions are convoluted by Fermi-Dirac distribution function and the Gaussian representing the resolution broadening of 300 meV. The comparison is shown in Figs. 4(e) and 4(f). The spectral shape corresponding to $U=0.6\pm0.1$ exhibits remarkable representation of the experimental bulk spectra in both the cases. These results clearly establish that perturbative approaches and local description of the correlation effects are successful in capturing electronic structure of these weakly correlated systems. The overall narrowing of the valence band observed in the substituted compounds is essentially a single-particle effect and can be attributed to the reduced degree of Ru-O-Ru connectivity in these systems. While the high energy scale features are reproduced remarkably well within this picture, the occurrence of a pseudogap at ϵ_F with increasing x (not visible in Fig. 4 due to large energy scale) suggests increasing role of disorder.

IV. CONCLUSIONS

In summary, the high resolution spectra of $SrRuO_3$ exhibit signature of disorder in the vicinity of the Fermi level. Ti substitution influences the spectral line shape of the bulk spectra and a dip appears at ϵ_F (pseudogap). First principles approaches are found to be sufficient to capture the bulk spectra, and U remains almost the same across the series. The effects are much stronger in the (two-dimensional) surface electronic structure, leading to a soft gap at 50% substitution and eventually a hard gap appears. Thus, this study provides an example where a metal-insulator transition is observed in two dimensions as a function of local potential keeping the electron correlation strength U unchanged as studied within the ionic Hubbard model.

*Corresponding author: kbmaiti@tifr.res.in

[1] A. Fuhrmann, D. Heilmann, and H. Monien, Phys. Rev. B **73**, 245118 (2006).
[2] S. S. Kancharla and E. Dagotto, Phys. Rev. Lett. **98**, 016402 (2007).
[3] Arti Garg, H. R. Krishnamurthy, and Mohit Randeria, Phys. Rev. Lett. **97**, 046403 (2006).
[4] N. Paris, K. Bouadim, F. Hebert, G. G. Batrouni, and R. T. Scalettar, Phys. Rev. Lett. **98**, 046403 (2007).
[5] K. W. Kim, J. S. Lee, T. W. Noh, S. R. Lee, and K. Char, Phys. Rev. B **71**, 125104 (2005).
[6] R. S. Singh and K. Maiti, Solid State Commun. **140**, 188 (2006).
[7] G. Cao, S. McCall, M. Shepard, J. E. Crow, and R. P. Guertin, Phys. Rev. B **56**, 321 (1997).
[8] K. Maiti and R. S. Singh, Phys. Rev. B **71**, 161102(R) (2005).
[9] K. Maiti, Phys. Rev. B **73**, 235110 (2006).
[10] J. Kim, J.-Y. Kim, B.-G. Park, and S.-J. Oh, Phys. Rev. B **73**, 235109 (2006), M. Abbate, J. A. Guevara, S. L. Cuffini, Y. P. Mascarenhas, and E. Morikawa, Eur. Phys. J. B **25**, 203 (2002).
[11] M. Takizawa, D. Toyota, H. Wadati, A. Chikamatsu, H. Kumigashira, A. Fujimori, M. Oshima, Z. Fang, M. Lippmaa, M. Kawasaki, and H. Koinuma, Phys. Rev. B **72**, 060404(R) (2005).
[12] K. Maiti, R. S. Singh, and V. R. R. Medicherla, Europhys. Lett. **78**, 17002 (2007).
[13] B. L. Altshuler and A. G. Aronov, Solid State Commun. **30**, 115 (1979).
[14] D. D. Sarma, A. Chainani, S. R. Krishnakumar, E. Vescovo, C. Carbone, W. Eberhardt, O. Rader, Ch. Jung, Ch. Hellwig, W. Gudat, H. Srikanth, and A. K. Raychaudhuri, Phys. Rev. Lett. **80**, 4004 (1998).
[15] A. L. Efros and B. I. Shklovskii, J. Phys. C **8**, L49 (1975).
[16] J. G. Massey and M. Lee, Phys. Rev. Lett. **75**, 4266 (1995).
[17] K. Maiti, P. Mahadevan, and D. D. Sarma, Phys. Rev. Lett. **80**, 2885 (1998).
[18] K. Maiti, D. D. Sarma, M. J. Rozenberg, I. H. Inoue, H. Makino,

O. Goto, M. Pedio, and R. Cimino, Europhys. Lett. **55**, 246 (2001).
[19] K. Maiti and D. D. Sarma, Phys. Rev. B **61**, 2525 (2000).
[20] K. Maiti, Ashwani Kumar, D. D. Sarma, E. Weschke, and G. Kaindl, Phys. Rev. B **70**, 195112 (2004).
[21] P. Blaha, K. Schwarz, G. K. H. Madsen, D. Kvasnicka, and J. Luitz, *WIEN2k: An Augmented Plane* Wave+Local *Orbitals Program for Calculating Crystal Properties* (Technische Universität Wien, Austria, 2001).
[22] G. Treglia, F. Ducastelle, and D. Spanjaard, J. Phys. (Paris) **41**, 281 (1980); Phys. Rev. B **21**, 3729 (1980); D. D. Sarma, F. U. Hillebrecht, W. Speier, N. Martensson, and D. D. Koelling, Phys. Rev. Lett. **57**, 2215 (1986).